IGNEOUS PROCESSES ON THE MOON AS SEEN IN NORTHWEST AFRICA 12384: A LUNAR MARE BASALT BRECCIA PUZZLE. C. J.-K. Yen[1], P. K. Carpenter[1], A. J. Irving[2], and B. L. Jolliff[1], [1]Dept. of Earth and Planetary Sciences and the McDonnell Center for the Space Sciences, Washington University, St. Louis, MO, USA (yenc@wustl.edu), [2]Dept. of Earth & Space Sciences, University of Washington, Seattle, WA, USA.

Introduction: Northwest Africa (NWA) 12384 was recovered in 2018 in Mali and was classified as a lunar mare basalt breccia [1, 2]. Carpenter et al. (2019a) and Carpenter et al. (2019b) studied the petrology and bulk composition of several clasts in an end-cut (EC-1) of the meteorite. They also mapped a portion of the main basalt clast using quantitative methods and tested for petrogenetic relationships between clasts. Following those studies, we analyzed a center-cut polished thin section (PTS-1) of NWA 12384 using similar methods and present the crystallization and cooling history as suggested by the texture, mineralogy, and petrography of the meteorite. This lunar meteorite in one sample represents different stages of magmatic differentiation and offers an additional way to study petrogenetic processes on the Moon.

Volcanism on the Moon has been studied through Apollo and meteorite sample analyses, remote sensing, and crystallization models. Lunar mare volcanism on a simplified scale involves magma reservoirs, magma conduits, lava flows, and pyroclastic materials [3, 4]. Mare basalts are produced by partial melting of the Moon's mantle and thus are valuable samples for studying the Moon's interior, which is otherwise inaccessible to researchers. Numerous precious samples returned by the Apollo missions from a limited region of the Moon, combined with the diverse array of lunar meteorites, allow for more comprehensive studies of lunar geology [5]. A sample such as NWA 12384, with several distinct clast lithologies in one rock, is an opportunity to test for petrogenetic relationships and whether different breccia components represent different stages of lunar mare volcanism. In addition, comparisons with analyses of Apollo basalt samples may offer clues to the general origin of NWA 12384.

We identified 27 distinct clasts in PTS-1 (Fig. 1) with backscattered-electron mosaic imaging and X-ray intensity mapping using an AlMgFe RGB map. Of primary interest in this study are clasts 2 and 3. Furthermore, several picritic glass beads were identified and used as primary compositions for crystallization models. Clast 2 was studied for possible petrogenetic relations with the large main basalt clast, clast 3, owing to textural and phase similarities. Clast 3 is the largest clast in the thin section and is a pigeonite basalt with soda-straw pyroxene phenocrysts that zone from pigeonite to augite and contain little "augen" of plagioclase at their cores. The groundmass of clast 2 is finer grained compared to that of clast 3, but both consist predominantly of pyroxene, plagioclase, ilmenite, and minor phases such as ulvöspinel, chromite, and silica. We used EPMA spot analyses and quantitative compositional mapping to determine the mineral chemistry and bulk chemistry of clasts, then used the results to study petrogenetic relationships and igneous processes among these basaltic clast lithologies.

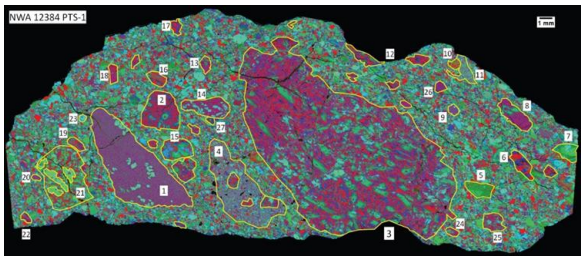

Figure 1. *AlMgFe X-ray map of PTS-1 with clast outlines. The quantitative compositional map is of basalt clast 3.*

Methods: We analyzed the minerals in PTS-1 with a JEOL JXA-8200 electron microprobe at Washington University equipped with 5 WDS detectors and 1 SDD for EDS. Spot analyses were made with WDS with an accelerating voltage of 15 kV and a beam current of 25 nA. The spot size was typically 3 μm, but occasionally 20 μm and 1 μm spots were used to defocus for a bulk composition and focus for small features, respectively. Chemistry of minerals such as olivine, pyroxene, and plagioclase were plotted to visualize spatial trends, for example, within a phenocryst versus the matrix (Fig. 2).

Quantitative EPMA maps were made of the main basalt clast 3 using methods described in [1]. These element wt. % images were processed in MATLAB and analyzed in the Environment for Visualizing Images (ENVI) software. We ran a supervised classification using Spectral Angle Mapper (SAM) and a spectral library made using data from [1] to create a classification map (Fig. 3). SAM calculates the angle between the spectra of a pixel and that of a reference in n-Dimensional space, where n corresponds to the number of bands. In this case, there were 10 "bands" that corresponded to Na, Mg, Al, Si, K, Ca, Ti, Cr, Mn, and Fe wt. %. We used the combined chemistry and the spatial map to reconstruct the bulk composition of basalt clast 3. SAM was also used successfully to locate other picritic glass beads similar in chemistry to the large one.

The bulk composition of the two clasts were compared with the meteorite bulk composition from [1] as well as those of Apollo samples. Potential petrogenetic relationships were tested using the FXMOTR equilibrium-and-fractional crystallization

model in SPICES [6]. A large (~1 mm long-axis) picritic glass bead in PTS-1 was tested as an assumed starting composition to determine a liquid line of descent along which the basaltic lithologies may have formed. FXMOTR model was run at 1 bar and 1 kbar using the large picritic glass bead composition as the initial melt.

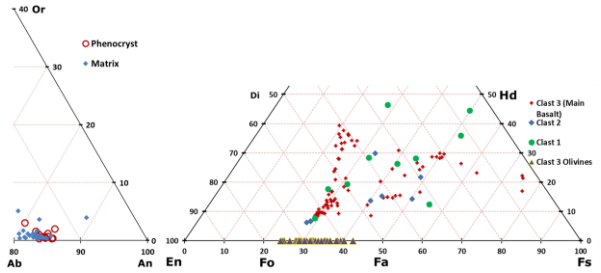

Figure 2. *Plagioclase compositions in the pyroxene phenocrysts and the groundmass of clast 3 (left), and various pyroxene compositions show zoning from pigeonite to augite in phenocrysts and more Fe-rich groundmass (right). Clast 3 olivine phenocryst compositions are shown along the base axes, with most having compositions of* Fa_{29} *(core) or* Fa_{37} *(rim).*

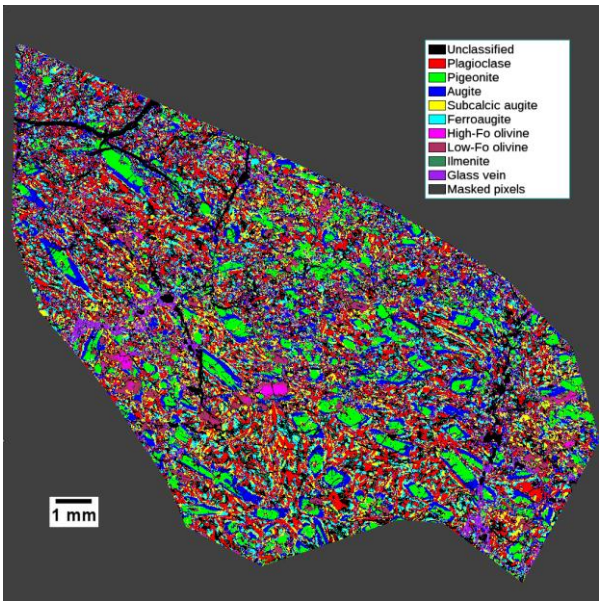

Figure 3 *SAM classification map for basalt clast 3.*

Results and Discussion: The estimated mineral proportions in area percent of clast 3 from the SAM classification map is 25% plagioclase, 15% pigeonite, 19% augite, 19% subcalcic augite, 15% ferroaugite, 6% olivine, and 1% ilmenite (Fig. 3). CIPW normative calculations (wt. %) of this chemistry result in 26% plagioclase, 0.5% orthoclase, 27% diopside, 32% hypersthene, 11% olivine, 3% ilmenite, and 0.6% chromite. We estimate the phenocryst to matrix area proportion of clast 3 to be roughly 20:80%. Modal recombination of the two clasts show similar compositions to the meteorite bulk composition and basalt clast bulk recalculation from [1] (Table 1).

	Clast 3 pigeonite basalt	Clast 2 basalt	Bulk meteorite from [1]	Basalt Clast Bulk Recalc. from [1]	12009	NWA 12384 Glass Bead Average	A15 Green D [8]
SiO2	46.35	48.95	45.25	45.60	45.03	44.78	45.00
TiO2	1.59	0.52	2.00	2.70	2.90	0.77	0.40
Al2O3	8.76	11.33	7.51	8.82	8.59	6.67	7.37
Cr2O3	0.38	0.47	0.30	0.55	0.55	0.51	0.50
FeO	18.56	16.53	20.43	20.32	21.03	20.34	20.57
MnO	0.25	0.27	0.28	0.27	0.28	0.27	0.27
MgO	11.07	10.84	13.98	11.32	11.55	18.62	18.30
CaO	10.78	9.70	9.81	9.70	9.42	7.21	8.25
Na2O	0.47	0.51	0.40	0.40	0.23	0.13	0.20
K2O	0.08	0.05	0.01	0.08	0.06	0.03	N/A
Total	98.3	99.2	100.0	99.8	99.6	99.3	100.9
Mg#	51.5	53.9	55.0	49.8	49.5	62.0	61.3

Table 1. *Bulk compositions of mineral phases for clasts in PTS-1, compared with EC-1 meteorite bulk composition and main basalt clast from [1], as well as volcanic glass bead data.*

Comparisons of major element compositions of the bulk compositions of clast 3 in PTS-1 and the main basalt clast in EC-1 [1] with Apollo basalt samples show the closest match with Apollo 12 and 15 olivine and pigeonite basalts. One of the most similar Apollo samples with respect to major elements is 12009, which is an olivine vitrophyre and therefore texturally very different. Texturally, the descriptions of oscillatory zoning and plagioclase-Fe-rich clinopyroxene-ilmenite aggregate cores in pyroxene phenocrysts of Apollo 12 basalts 12021 and 12052 are similar to those observed in the basalt clast 3 of PTS-1 [e.g., 7], and the pyroxene compositional trends are analogous although the bulk compositions are not as similar as that of 12009. The plagioclase cores of the pyroxenes likely formed from trapped melt as the hollow phenocrysts crystallized. The pyroxene compositions are consistent with previous work, and support at least two distinct cooling stages, slow (at depth) and rapid (on eruption) [1, 9]. We also observe an apparent alignment of the pyroxene phenocrysts in clast 3 consistent with the multi-stage cooling model, as was also concluded previously [7].

Fourteen spot analyses across the large picritic glass bead revealed a homogeneous composition which is in the VLT range and closest to those of Apollo 15 Green D and Apollo 14 Green B [8]. Crystallization model results indicate the two clasts are not direct derivatives of the volcanic glass bead as there are similar, but no common liquid lines of descent. The bulk compositions of clast 2 and basalt clast 3 could not be directly derived by olivine subtraction from that of the volcanic glass, owing to lower Fe content and differences in incompatible elements such as Ti and Cr. From the meteorite bulk composition and the apparent lithology of clasts in PTS-1 and EC-1, there does not appear to be significant incorporation of nonmare components.

References: [1] Carpenter, P. et al. (2019a) *LPS L*, Abstract #2148. [2] Carpenter, P. et al. (2019b) *LPS L*, Abstract #2125. [3] Head, J. and Wilson, L. (1992) *GCA, 56*, 2155–2175. [4] Housley, R. (1978) *LPS IX*, 1473–1484. [5] Korotev, R. (2005) *Chem. Erde, 65*, 297–346. [6] Davenport, J. et al. (2014) *LPS XLV*, Abstract #1111. [7] Bence, A. et al. (1971) *LPS II*, 559–574. [8] Shearer, C. and Papike, J. (1993) *GCA, 57*, 4785–4812 [9] Bence, A., and Papike, J. (1972) *LPS III*, 431–469.